

Joana Reis^{1*}, Teresa Oliveira², Alfredo Pereira³, Paulo Infante⁴, Nuno Leal⁵, Pedro Faísca⁶

¹ Departamento de Medicina Veterinária - Escola de Ciências e Tecnologia
Universidade de Évora

² Departamento de Medicina Veterinária - Escola de Ciências e Tecnologia
Instituto de Ciências Agrárias e Ambientais Mediterrânicas, Universidade de Évora

³ Departamento de Zootecnia - Escola de Ciências e Tecnologia
Universidade de Évora

⁴ Departamento de Matemática - Escola de Ciências e Tecnologia
Centro de Investigação em Matemática e Aplicações / IIFA
Universidade de Évora

⁵ DNAtch Laboratório Veterinário; Hospital Veterinário do Oeste

⁶ Centro de Investigação em BioCiências e Tecnologias da Saúde, Faculdade de Medicina Veterinária-
Universidade Lusófona de Humanidades e Tecnologias/ DNAtch Laboratório Veterinário

*Corresponding author: Joana Reis

Email address: jmfcr@uevora.pt

Orcid:0000-0002-9910-2036

Veterinary Medicine Department
School of Sciences and Technology
University of Évora

Correspondence:

Joana Reis

Departamento de Medicina Veterinária

Escola de Ciências e Tecnologia - Universidade de Évora

Polo da Mitra - Apartado 94

7002-554 Évora

Portugal

Running title: *Calcifications in canine mammary tumours*

Acknowledgments: This work has been partially supported by the European Commission through Portugal 2020/Alentejo 2020, grant POCI-01-0145-FEDER-032486.

The authors thankfully acknowledge Professor Rita Payan Carreira (Universidade de Évora) for kindly reviewing the manuscript and to Dr Nuno Pinheiro da Silva, MD (Hospital de S. João, Porto) for reviewing the microcalcifications' classification. The authors are also grateful to the veterinary medicine students that volunteered some of their time to help with part of the procedures: Daniela Pinto, Carina Linhares, Bárbara Santos, Ana Isabel Neto and Carolina Gusmão, amongst others. The authors thank Inês Carvalho (DNATech Laboratório veterinário) and Marta Brito and Luisa Fialho (Universidade de Évora) for technical support.

This article has been accepted for publication and undergone full peer review but has not been through the copyediting, typesetting, pagination and proofreading process, which may lead to differences between this version and the Version of Record. Please cite this article as doi: 10.1111/vco.12545

Abstract: The present work describes the microtomographic characterization of macro and microcalcifications present in excised canine mammary glands. In human breast cancer, microcalcifications are highly relevant for diagnosis and prognosis, often being the sole element determining biopsy. Canine mammary tumours are considered a model for human breast cancer, but the morphological features of calcifications had still to be studied in this species. The objective of this research is to contribute to the characterization of the mineralization features of the canine mammary gland.

In the present study, the excised mammary glands of 33 bitches underwent fluoroscopic examination. In 30 of the samples, the presence of calcification was suspected, and multiple biopsies were taken of these areas. Biopsy fragments underwent microtomographic scanning. Microcalcifications were found in non-neoplastic glandular tissue, benign and malign lesions, as it is known to happen in humans. Qualitative evaluation regarding morphology of the imaged calcifications showed similarities to breast cancer findings, based on the BI-RADS 2013 classification, such as pleomorphism and shape. No differences in the quantitative morphological parameters of volume, surface, surface/volume, SMI and structure thickness were found when macrocalcifications were considered. However, although significant differences existed in these parameters between microcalcifications from malignant canine mammary tumours and the two other groups, none were found between non-neoplastic and benign tumours. Findings further support the use of this spontaneous animal model for the study of human breast cancer, considering how clinically relevant microcalcifications are in humans.

Keywords: Animal model; calcifications; canine mammary tumours; microcalcifications; microtomography.

1. Introduction

Calcium deposits within the mammary tissue are associated with diagnosis and prognosis of breast cancer in humans¹. The calcification morphology and distribution are determinant for clinical decisions such as the need for urgent biopsy, independently of the presence of palpable masses. Mineralization is thus very clinically relevant in human breast cancer. However, little is known about the mineralization processes in canine mammary tumours.

The American College of Radiology, in cooperation with other clinical organizations, developed a system to standardize mammography reports - the Breast Imaging Reporting and Data System (BI-RADS). A specific lexicon of imaging features was provided, and a scale developed². The system has been reviewed and updated³, and overall has shown its ability in predicting benignity and malignancy⁴. Its 5th edition has simplified calcification classification into two categories: typically benign and suspicious morphology^{4,5}.

In malignant lesions such as pre-invasive ductal carcinoma and invasive duct carcinoma, calcifications may follow the expanse of the duct, branching out, and may appear as long, irregular V or rod- shaped calcium deposits⁶. Fine linear calcifications are strongly correlated with malignancy, while large “pop-corn” or eggshell- like calcifications are suggestive of benignity. The morphological features of calcifications have also been correlated with the prognosis⁷⁻⁹. The obvious advantage is to avoid invasive procedures in benign lesions and to prompt biopsy and early diagnosis whenever malignancy is suspected.

Spontaneous canine invasive mammary carcinomas have been considered as a model for human breast cancer based on high incidence, risk factors, age of onset and biological and metastatic behaviours, with similar gene expression patterns¹⁰⁻¹³. Canine mixed mammary tumours have also been evaluated as a model for human breast cancer with osseous metaplasia¹⁴. Canine inflammatory mammary carcinoma has also been suggested as a model for human inflammatory breast cancer¹⁵. One study, conducted in 40 bitches submitted to mastectomy, affirmed that mammographic findings in pre-invasive, benign and malign lesions are similar to those in humans, enabling the application of the BI-RADS system to mammary tumours in dogs. The authors describe a mammography diagnostic sensitivity of 90% and specificity of 82.8%¹⁶. Several studies of the ultrasound characterization of canine mammary tumours are also available, underlining similarities to human disease, dependent on the criteria under consideration¹⁶⁻¹⁸.

Digital fluoroscopy has not been used for detection of canine mammary tumour calcification, but in this study, it enabled the collection of real-time image-guided biopsies in large samples such as mammary chains.

Micro-computed tomography (microCT) was applied to characterize microcalcifications in biopsies taken from radiographically suspicious breast lesions in women, correlating findings with the anatomopathological results¹⁹⁻²¹.

The present research describes preliminary microCT characterization of micro and macrocalcifications in biopsies from excised canine mammary glands, correlating the qualitative and quantitative results with the histopathological findings. To the authors' knowledge, no such study has so far been published.

The goal of this research is to contribute to knowledge and critical analysis of canine mammary tumours as a spontaneous model of human disease as regards the mineralization processes.

2. Materials and methods

2.1. Samples

Mammary glands from 33 female dogs were excised by regional or complete mastectomy and fixed in 10% buffered formalin. The mastectomies were performed by different surgeons in routine practice from November 2017 to April 2018. All tissues were identified by a randomized alphanumeric code.

The mammary glands were routinely processed for histopathology diagnosis: tissue from mammary tumours present in mammary glands was collected and routinely processed for paraffin embedding, sectioned into 3 μm slides and stained with hematoxylin-eosin. Mammary tumours were classified according to the Goldschmidt et al. proposal²² to an adaptation of the Elston and Ellis grading system developed by Peña et al. (2013) for canine mammary tumours²³. Malignant lesions were identified in 13 of the 33 animals (39.4%). Results from the initial histopathological analysis for the 33 samples are summarized in Table 1.

The remaining mammary gland segments, herein referred to as samples, were then submitted to imaging and biopsy and kept in formalin in between procedures. Biopsy histopathology was performed after the microCT scanning.

2.2. Imaging

2.2.1. Fluoroscopy

All the samples were imaged by fluoroscopy (Zen-2090 Pro, Genoray, Gyeonggi-do, Korea) and the images recorded. Whenever there was even slight suspicion of the presence of calcifications, a biopsy was taken from the area, using an 8mm punch, identifying each fragment and the exact place of collection. The sole criterion for biopsy was suspicion of calcification due to increased radiopacity. If several different areas of a given sample were suspected of presenting calcifications, multiple fragments were collected. Only 30 of the 33 early specimens showed areas of radiopacity high enough to arouse suspicion; in three of the samples, there was no suspicion of mineralization.

2.2.2. Microtomography

A total of 63 biopsies were taken from 30 samples and underwent microCT scanning (Skyscan 1174, Kontich, Belgium). The biopsy fragments were rinsed with distilled water to remove excess formalin and coated with Parafilm M[®] (Sigma Aldrich, Missouri, USA) to avoid sample dehydration during scanning. Subsequently, these fragments were placed in a rotation stage fixed by commercial play-dough. Scans were performed with 33-kVp, 403- μ A and an 0.25-mm aluminium filter. The pixel size was 31.04 μ m, the exposure time 2,200 ms, the rotation step 0.7° and the full rotation over 360°, with three average frames per image. Each fragment went through one scan, lasting approximately 89 minutes. After scanning, the fragment was again immersed in formalin.

The cross-section images were reconstructed using N-Recon software (Skyscan, Kontich, Belgium). All the samples underwent a complete analysis in the analysing software (CTAn, Skyscan, Kontich, Belgium). For each positive sample, an average of 8 microcalcifications (< 1 mm) were randomly chosen, when present, and a volume of interest (VOI) was defined for each microcalcification. The following parameters were evaluated for each database: object volume (Obj.V – mm³), object surface (Obj.S – mm²), object surface/volume ratio (Obj.S/Obj.V – 1/mm), structure model index (SMI), structure thickness (St.Th – mm) and object number (Obj.N). A uniform threshold method was applied.

After the CTAn analysis, all the samples were 3D-reconstructed in CTVox (CTVox, Skyscan, Kontich, Belgium) to compare their calcifications' morphology qualitatively.

2.3. Histopathology

The biopsy fragments were kept in buffered formalin and routinely processed for paraffin embedding after the microCT. Due to mineralization, six of the fragments had to be decalcified before embedding, using RDO. Every biopsy was sectioned in two to three longitudinal segments, placed side by side, before embedding. RDO was also used on blocks as necessary for sectioning. Blocks were sectioned into at least five 3 µm slides and stained with hematoxylin-eosin, alizarin red, and Von Kossa. Neoplastic lesions were classified according to the criteria defined in section 2.1.

2.4. Statistical analysis

Due to non-normal distribution, the Kruskal-Wallis nonparametric test was chosen, since in all cases the form of the distribution of the groups was similar. If there were significant differences between groups, comparisons were made by the Dunn test, with p-values adjusted by Sidák correction. All tests were performed using the NCSS 11 software package.

3. Results

Calcified lesions were confirmed by microCT in 21 biopsies from 13 dogs.

Fluoroscopy was helpful in identifying the macrocalcifications detected in this study, later confirmed by micro CT (Figure 1). The image intensifier was used with the goal of better targeting the biopsy collection, not of characterizing the calcifications, although some of the images suggested irregular, branching patterns of calcification (Figure 1).

Macrocalcifications ($\geq 1\text{mm}$) were found in 9 biopsies from 5 dogs. Microcalcifications ($< 1\text{mm}$) totalling 122 objects were detected in 21 of the biopsy fragments, from 13 dogs. Benign and malignant mixed-type tumours accounted for 63.9% of the microcalcifications. The imaging results were then correlated with the histopathology findings in the biopsies. Of the 21 fragments with tomographically confirmed mineralization, nine were from benign tumours (42.9%), eight were from malignant tumours (38.1%) and four (19%) presented non-neoplastic, glandular tissue (Table 2). It was possible to confirm by microscopy the mineral deposits in most of the biopsies.

Qualitatively, in the microCT three-dimensional (3D) reconstructed images of macrocalcifications, differences were apparent between malignant and benign lesions.

Macrocalcifications present in malignant lesions appeared as clusters of pleomorphic,

needle-like or branched, rod-like objects (Figure 2), while the macrocalcifications in benign lesions tended to appear as clusters of spherical or popcorn-like objects (Figure 3a and 3b). These differences were not evident in all surfaces of the larger objects.

The qualitative evaluation of microcalcifications' 3D rendered images followed the same pattern, with multiple or single spherical objects in non-neoplastic and benign tumours (Figure 4a) and the suggestion of more heterogeneous, rod-like shapes in malignant lesions (Figure 4b). However, a few of the microcalcifications had intermediate shapes, with part of the mineralization in non-neoplastic tissue and benign tumours presenting rod-like shapes while some were close to teacup shapes (Figure 5a and 5b).

Table 3 overviews the 3D quantitative parameters of the calcifications as averaged for each sample, including macro and microcalcifications, divided into malignant tumours, benign tumours and non-neoplastic lesions. As data from all calcifications were included, a larger variation was expected.

The presence of macrocalcifications was not related to malignancy, but no macrocalcifications were found in the four fragments with non-neoplastic tissue. The results from the quantitative morphological parameters (Obj.V, Obj.S, Obj.S/Obj.V, SMI and St.th) were compared according to the classification as malign, benign or non-neoplastic. No statistically significant differences between malignant and benign groups were found when macrocalcifications were included in the dataset. SMI was significantly different in the non-neoplastic group calcifications.

The 3D morphology parameters of the 122 isolated microcalcifications were also analysed, as summarized in Table 4. Of these, 59 were in fragments from benign tumours, 24 microcalcifications in non-neoplastic glandular tissue and 39 in malignant

lesions. Groups were compared using the Dunn test, with p-values adjusted by Sidák correction. No significant differences were found between the microcalcifications in benign and non-neoplastic groups, but they were found ($p < 0.05$) between the above groups and malignant tumours relating to all morphological parameters: Obj.V, Obj.S, Obj.S/Obj.V, St.Th and SMI. The microcalcifications' mean volume was approximately ten times higher in the malignant tumours than in the benign and non-neoplastic ones. The microcalcifications' median volume was almost four times higher in malignant lesions. Corresponding mean and median surface and structure thickness were higher in malignant lesions (Figure 6). In this study, 63.9% of the microcalcifications were found in mixed-type tumours (69.2% of these in benign mixed tumours and 30.8% in carcinoma mixed-types). Microcalcification mean volume was significantly different between these two types but not so when carcinoma mixed-type tumours were compared with the other malignant tumours. Microcalcifications in non-neoplastic tissue did not differ significantly from those in benign mixed tumours and the other benign tumour fragments. Besides mixed-type tumors, mineralization was also found in complex adenomas and carcinomas, comedocarcinomas and in non-neoplastic glandular tissue. In these, mineralization was observed in areas of necrosis and sclerosis (Figure 7), normal or hyperplastic glandular tissue, as well as in the internal elastic lamina of muscular arteries walls (Figure 8).

4. Discussion

Being aware of the relatively low sensitivity (52%) of fluoroscopy in terms of detecting coronary calcification in humans²⁴, and of the different degrees of x-ray beam

attenuation produced by the differences in sample constitution and thickness and the possible sub-millimetric calcifications, the authors opted to take biopsies of the areas showing increased radiopacity. As a result of this overcautious approach, microcalcifications were confirmed by microCT in approximately 33% of the fragments taken under fluoroscopy. The microCT 3D rendered images were analysed qualitatively and quantitatively and the results correlated with the histopathological results. MicroCT 3D imaging has been applied to human breast biopsies to characterize microcalcifications present in benign and malignant lesions,¹⁹⁻²¹ but so far no microCT data on canine mammary tumour calcifications is available. Microtomography is applicable to small scale samples, with high resolution. It has limited application in a clinical practice context, mainly due to the length of time needed for a single scan (89 minutes in the present study) and sample size limitations. At the most, some equipment allows in vivo scanning of small rodents and rabbit limbs. Computational power needs must also be pondered in larger samples with a high resolution. However, microCT has proved an invaluable imaging tool in biomedical research, and in this study, it was used to explore the mineralization processes in the canine mammary gland, on a submillimetric scale. Conventional CT scanners do not allow such high resolutions. Mammograms are not routine in small animal practice, and there are very few reports on their use with regard to dogs. A previous study described similarities between calcifications in benign and malignant tumours in dogs, with the application of BI-RADS categories to canine disease.¹⁶ However, the mammograms were undertaken in excised mammary glands, so clinical applicability is uncertain.

In dogs, partial, regional or radical mastectomy is standard procedure in the presence of mammary tumours. The heterogeneity of canine mammary tumours renders aspiration

cytology an unreliable tool. Benign lesions exfoliate fewer cells, and samples may not be diagnostic; tumour size may also interfere with the ability to collect a representative sample unless ultrasound guidance is used ²⁵. Malignant tumours may be underdiagnosed by cytology, leading to low sensitivity ²⁶. Non-excisional biopsies are rarely performed, and mastectomy remains standard practice, although nodulectomy is sometimes carried out.

In the present study, microcalcifications were found in non-neoplastic glandular tissue, in benign tumours and in malignant tumours, as is also described in the human breast; although four of the fragments consisted of non-neoplastic tissue, macrocalcifications were identified only in benign and malign lesions. When the number of calcifications were compared, no differences were found between benign and malignant lesions.

The methodology followed in this study is distinct from the two previous microCT studies conducted in human breast cancer biopsies ^{6,20,21} because the only criterion determinant for fragment collection in the current study was suspected mineralization, regardless of its pattern. Clinical aspects such as size, growth rate, limits or consistence/presence of palpable mass were not considered in the collection of biopsies. As a result, no bias was introduced by the level of suspicion of malignancy.

The qualitative evaluation of the calcifications, taking the shape into account, suggested similarities to findings in malignant and non-neoplastic/ benign lesions in human breast cancer. However, some intermediate shapes were found that could lead to misdiagnosis.

A non-parametric, conservative statistical test was chosen to compare groups with regard to quantitative variables, in order to ensure that the differences among these groups were not artefactual.

Microcalcifications from malignant lesions were significantly different from the ones found in benign lesions and non-neoplastic tissue, for all tested variables. Microcalcifications from malignant tumours had a significantly higher volume, surface, and a significantly lower object surface/ volume ratio, unlike those in the previous studies of human breast biopsies^{20,21}. A lower surface/volume ratio might suggest that microcalcifications from malignant lesions were closer to a spherical shape (when qualitative evaluation suggests otherwise). However, since the surface/volume ratio is inversely proportional to volume, a nearly ten-fold increase in average volume in objects from malignant lesions did not translate into a proportional decrease in surface/volume ratio. Therefore, such an assumption cannot be made.

In the present study, although significant differences in SMI were found when malignant lesions were compared with non-neoplastic lesions, all groups have average values close to 3, which accords with findings in human biopsies^{20,21}. Since SMI is dependent on volume as well as on concave surfaces, the statistically significant differences may again be influenced by differences in volume and the shape of the object, especially when a concave surface is present, so care must be taken when interpreting this index²⁷.

In this study, 63.9% of the microcalcifications were found in mixed-type tumours (both benign and malignant) common in dogs, and containing cartilaginous and/or osseous tissue²². Our sample included six fragments in which a mixed benign tumour was

diagnosed, from five different animals. Four other fragments presented mixed type carcinoma, with chondroid and/or osseous metaplasia. Mixed-type tumours are common in dogs, while metaplastic breast cancer is quite rare in humans. Canine mixed tumours and metaplastic breast cancer share similarities concerning histopathological findings and molecular expression¹⁴. Most of the microcalcifications in this study were found in mixed-type tumours, identified in nearly half of the total number of fragments with calcification. This is different to what is found in women. However, the volume of the microcalcifications did not significantly differ between the mixed and non-mixed malignant fragments. Significant differences in volume were also found between microcalcifications present in malignant lesions, both mixed-type and non-mixed, and non-neoplastic and benign mixed lesions.

The heterogeneity of the sample in terms of the specific tumour type contributed to dispersion when these data subsets were considered. However, after microcalcifications have been taken into account, the results, divided into non-neoplastic, benign and malignant, are especially relevant, precisely because the sample is varied and representative of the diversity of this neoplastic disease in dogs.

Initial studies in human breast biopsies suggested microCT had good sensitivity (98%) in the detection of malignant lesions, but the specificity needed improvement (40%),¹⁹ and malignant lesions tended to present significantly higher numbers of microcalcifications, with smaller volume and higher object surface to volume ratio. SMI values were close to 3 and no significant differences were present between the two groups, totalling eleven samples²⁰. A more recent study, with 29 samples, using a higher isotropic spatial resolution of 9 μm (previous studies used a 35 μm spatial resolution),

found no significant differences between microcalcifications from malignant and benign lesions in morphological parameters; SMI was not useful for differentiating between malignant and benign tumours, but there are limitations inherent to this index, due to the way in which it is determined²¹. Differences in results between this study and the two previous ones in human breast biopsies may in part reflect the different criteria which apply to biopsies. Biopsies of the human breast were taken when malignancy was suspected, whilst in the present research the biopsies depended only on increased radiopacity.

The present study also used equipment with a lower resolution than previous breast cancer studies, limiting the capacity to detect and characterize smaller objects. The maximum resolution possible was used, with a pixel size of 31.04 μm , a 360° object rotation with 0.7° intervals and three frames average per image to optimize image quality.

It was decided not to exclude calcifications based on size. All available data was considered, taking calcifications with under 1 mm as a subset, due to their clinical relevance in breast cancer diagnosis.

The results show that malignancy in canine mammary tumours generates differences in the morphology of microcalcifications but not in macrocalcifications, suggesting different events in mineral deposition and growth. In breast cancer, differences in the chemical composition of the microcalcifications, dependent on tumour grade, has already been described²⁸.

The results of the current study support the hypothesis of an existing aberrant mineralization pathway in canine mammary tumours, dependent on malignancy and

distinct from physiological mineralization, as has already been suggested by the three-dimension culture of MCF10A human breast tumour progression series cell studies ²⁹. These authors observed mineralization in viable cell areas, directly correlated with malignancy potential, both in density and volume, in the absence of exogenous induction of osteogenic differentiation. Similar conclusions were drawn by a recent study, reporting heterogeneous matrix, matrix mineralization patterns and chemical composition of microcalcifications in breast cancer, in the absence of any evidence of an osteogenic pathway ³⁰. We hypothesize that a similar process may occur in malignant canine mammary tumours. Even in the mixed-type tumours, where mineralization occurred in the areas of osseous metaplasia, differences between malignant and benign tumours were significant and followed the same trend.

It is also possible that as neoplasms grow, other mineralization pathways are activated, due to mesenchymal differentiation and cell apoptosis ^{31,31,32}, explaining why no significant differences were found when calcifications larger than 1mm were considered.

Further research is necessary, with ampler sampling and complementary microtomographic data with the evaluation of mineralization, inflammation and apoptosis pathways through immunohistochemistry and molecular biology techniques.

In conclusion, the present study found significant differences in microcalcifications in malignant canine mammary tumours when compared to non-neoplastic glandular tissue and benign tumours, but not between the latter two groups. These results indicate that microcalcification morphology in the canine mammary gland changes according to the extent of malignancy, as is recognized in humans. The results and literature review also

revealed that little is known of the events that lead to mineralization in both species, despite its recognized clinical relevance in humans.

The results support the further use of this spontaneous animal model to study human breast cancer.

Conflict of Interest Statement

The authors declare that they have no conflicts of interest.

Data Availability Statement

The dataset supporting the conclusions of this article was generated in this study. It may be made available upon reasonable request to the corresponding author.

References

1. Cox RF, Morgan MP. Microcalcifications in breast cancer: Lessons from physiological mineralization. *Bone*. 2013;53(2):437-450.
2. D'Orsi CJ. The American College of Radiology mammography lexicon: an initial attempt to standardize terminology. *AJR American journal of roentgenology*. 1996;166(4):779-780.
3. Baker JA, Kornguth PJ, Floyd Jr C. Breast imaging reporting and data system standardized mammography lexicon: Observer variability in lesion description. *AJR American journal of roentgenology*. 1996;166(4):773-778.
4. Orel SG, Kay N, Reynolds C, Sullivan DC. BI-RADS categorization as a predictor of malignancy. *Radiology*. 1999;211(3):845-850.
5. D'Orsi CJ SEMEME et al. *ACR BI-RADS® Atlas, Breast Imaging Reporting and Data System*. 5th ed. American College of Radiology, Reston, VA; 2013.
6. Gary M, Tan PH, Pang AL, Tang AP, Cheung HS. Calcification in breast lesions- pathologists' perspective. *Journal of clinical pathology*. 2007.
7. Thurfjell E, Thurfjell MG, Lindgren A. Mammographic finding as predictor of survival in 1-9mm invasive breast cancers. Worse prognosis for cases presenting as calcifications alone. *Breast cancer research and treatment*. 2001;67(2):177-180.
8. Rominger MB, Steinmetz C, Westerman R, Ramaswamy A, Albert U-S. Microcalcification-Associated Breast Cancer: Presentation, Successful First Excision, Long-Term Recurrence and Survival Rate. *Breast care*. 2015;10(6):380-385.
9. Qi X, Chen A, Zhang P, Zhang W, Cao X, Xiao C. Mammographic calcification can predict outcome in women with breast cancer treated with breast-conserving surgery. *Oncology letters*. 2017;14(1):79-88.
10. Ettlin J, Clementi E, Amini P, Malbon A, Markkanen E. Analysis of gene expression signatures in cancer-associated stroma from canine mammary tumours reveals molecular homology to human breast carcinomas. *International journal of molecular sciences*. 2017;18(5):1101.
11. Pinho SS, Carvalho S, Cabral J, Reis CA, Gärtner F. Canine tumors: a spontaneous animal model of human carcinogenesis. *Translational Research*. 2012;159(3):165-172.
12. Uva P, Aurisicchio L, Watters J, et al. Comparative expression pathway analysis of human and canine mammary tumors. *BMC genomics*. 2009;10(1):135.

13. Queiroga FL, Raposo T, Carvalho MI, Prada J, Pires I. Canine mammary tumours as a model to study human breast cancer: most recent findings. *in vivo*. 2011;25(3):455-465.
14. Saad E, Milley K, Al-Khan A, et al. Canine mixed mammary tumour as a model for human breast cancer with osseous metaplasia. *Journal of comparative pathology*. 2017;156(4):352-365.
15. Raposo TP, Arias-Pulido H, Chaher N, et al. Comparative aspects of canine and human inflammatory breast cancer. In: *Seminars in oncology*. Vol 44.; 2017:288-300.
16. Mohammed SI, Meloni GB, Parpaglia MLP, et al. Mammography and ultrasound imaging of preinvasive and invasive canine spontaneous mammary cancer and their similarities to human breast cancer. *Cancer Prevention Research*. 2011:canprevres-0084.
17. Feliciano M, Vicente W, Silva M. Conventional and Doppler ultrasound for the differentiation of benign and malignant canine mammary tumours. *Journal of Small Animal Practice*. 2012;53(6):332-337.
18. Tagawa M, Kanai E, Shimbo G, Kano M, Kayanuma H. Ultrasonographic evaluation of depth-width ratio (D/W) of benign and malignant mammary tumors in dogs. *Journal of Veterinary Medical Science*. 2016;78(3):521-524.
19. Temmermans F, Jansen B, Willekens I, et al. Classification of microcalcifications using micro-CT. In: *Applications of Digital Image Processing XXXVI*. Vol 8856.; 2013:88561B.
20. Willekens I, Van de Castele E, Buls N, et al. High-resolution 3D micro-CT imaging of breast microcalcifications: a preliminary analysis. *BMC cancer*. 2014;14(1):9.
21. Kenkel D, Varga Z, Heuer H, et al. A Micro CT Study in Patients with Breast Microcalcifications Using a Mathematical Algorithm to Assess 3D Structure. *PloS one*. 2017;12(1):e0169349.
22. Goldschmidt M, Peña L, Rasotto R, Zappulli V. Classification and grading of canine mammary tumors. *Veterinary pathology*. 2011;48(1):117-131.
23. Peña L, Andrés PD, Clemente M, Cuesta P, Perez-Alenza M. Prognostic value of histological grading in noninflammatory canine mammary carcinomas in a prospective study with two-year follow-up: relationship with clinical and histological characteristics. *Veterinary Pathology*. 2013;50(1):94-105.
24. Agatston AS, Janowitz WR, Hildner FJ, Zusmer NR, Viamonte M, Detrano R. Quantification of coronary artery calcium using ultrafast computed tomography.

- Journal of the American College of Cardiology*. 1990;15(4):827-832.
25. Pierini A, Millanta F, Zanforlin R, Vannozzi I, Marchetti V. Usefulness of cytologic criteria in ultrasound-guided fine-needle aspirates from subcentimeter canine mammary tumors. *Journal of Veterinary Diagnostic Investigation*. 2017;29(6):869-873.
 26. Allen SW, Prasse KW, Mahaffey EA. Cytologic differentiation of benign from malignant canine mammary tumors. *Vet Pathol*. 1986;23(6):649-55.
 27. Salmon PL, Ohlsson C, Shefelbine SJ, Doube M. Structure model index does not measure rods and plates in trabecular bone. *Frontiers in endocrinology*. 2015;6:162.
 28. Baker R, Rogers KD, Shepherd N, Stone N. New relationships between breast microcalcifications and cancer. *Br J Cancer*. 2010;103(7):1034-9. doi:10.1038/sj.bjc.6605873.
 29. Vidavsky N, Kunitake JA, Chiou AE, et al. Studying biomineralization pathways in a 3D culture model of breast cancer microcalcifications. *Biomaterials*. 2018.
 30. Kunitake JA, Choi S, Nguyen KX, et al. Correlative imaging reveals physiochemical heterogeneity of microcalcifications in human breast carcinomas. *Journal of structural biology*. 2018;202(1):25-34.
 31. Kim K. Apoptosis and calcification. *Scanning microscopy*. 1995;9(4):1137-75.
 32. Scimeca M, Giannini E, Antonacci C, Pistolese CA, Spagnoli LG, Bonanno E. Microcalcifications in breast cancer: an active phenomenon mediated by epithelial cells with mesenchymal characteristics. *BMC cancer*. 2014;14(1):286.

Table 1. Summary of the initial samples' histopathological diagnosis

<i>Individual</i>	<i>Type</i>	<i>Lesion /Grade</i>	<i>Number of biopsies taken</i>
#1	Benign	Complex adenoma	2
#2	Benign	Adenosis	6
	Malignant	Complex carcinoma, G II	
#3	Malignant	Solid carcinoma	4
#4	Benign	Benign mixed	2
#5	Malignant	Solid carcinoma, G III	4
#6	Benign	Complex adenoma	1
#7	Malignant	Simple carcinoma, G III	2
	Benign	Simple adenoma	
#8	Benign	Complex adenoma	1
#9	Malignant	Malignant mixed, G II	2
#10	Malignant	Solid carcinoma, G I	1
#11	Benign	Complex adenoma	2
#12	Malignant	Solid carcinoma, G III	1
#13	Malignant	Complex carcinoma, G II	2
#14	Malignant	Complex carcinoma, G I	2
#15	Benign	Benign mixed	3
#16	Benign	Complex adenoma	3
	Benign	Simple adenoma	

#17	Benign	Complex adenoma	1
#18	Malignant	Comedocarcinoma, G III	3
#19	Malignant	Malignant mixed, G III	1
#20	Benign	Adenosis	3
#21	Benign	Complex adenoma	3
	Benign	Benign mixed	
#22	Benign	Benign mixed	1
	Malignant	Complex carcinoma, G I	1
#24	Benign	Complex adenoma	4
#25	Benign	Adenosis	1
#26	Malignant	Solid carcinoma, G I	2
	Benign	Fibroadenoma	
#27	Benign	Complex adenoma	2
#28	Malignant	Complex carcinoma, G II	1
#29	Benign	Simple adenoma	1
#30	Benign	Complex adenoma	1
#31	Benign	Adenosis	0
#32	Benign	Complex adenoma	0
#33	Benign	Simple adenoma/ Simple carcinoma, G III	0

Table 2. Summary of histopathological findings in biopsy fragments with mineralization confirmed by microCT

<i>Individual Fragment</i>		<i>Histopathology</i>			<i>MicroCT</i>	
	<i>Type</i>	<i>Histopathology biopsy findings</i>		<i>Calcification location in section</i>	<i>Macrocalcifications</i>	<i>Microcalcifications</i>
#4	#1	Benign	Complex adenoma	-		+
#5	#3	Malignant	Solid carcinoma	-		+
#9	#1	Malignant	Mixed carcinoma	Bone	+	+
	#3	Malignant	Mixed carcinoma	Bone	+	+
#11	#1	Non-neoplastic	Glandular tissue	Arterial wall, glandular tissue		+
	#2	Non-neoplastic	Glandular tissue	Glandular duct		+
#13	#1	Malignant	Mixed carcinoma	Bone	+	+
	#2	Malignant	Mixed carcinoma	Bone	+	+
#15	#2	Benign	Benign mixed	Bone		+
#17	#1	Benign	Benign mixed	Bone	+	+
#18	#1	Malignant	Comedocarcinoma	Necrosis foci		+
	#3	Malignant	Comedocarcinoma	Necrosis foci		+
#19	#1	Malignant	Neoplastic emboli, inflammation and non-neoplastic glandular tissue	Glandular tissue		+
#21	#1	Benign	Benign mixed	Bone	+	+
	#2	Benign	Benign mixed	Bone	+	+
	#3	Non-neoplastic	Glandular tissue	-		+
#24	#1	Benign	Benign mixed	Bone	+	+
	#2	Benign	Complex adenoma	Glandular tissue		+
	#3	Benign	Benign mixed	Bone	+	+
#25	#1	Non-neoplastic	Glandular sclerosis, stromal inflammation	Sclerosis foci		+
#27	#2	Benign	Complex adenoma, stromal inflammation	Multifocal, non-specific		+

Table 3. Summary 3D quantitative parameters of the calcifications as averaged for each sample, including macro and microcalcifications, considering malignancy. Note that no macrocalcifications were found in non-neoplastic fragments, as opposed to fragments showing benign and malign neoplastic changes.

<i>Malignancy</i>		<i>Volume</i>	<i>Surface</i>	<i>Surface/Volume</i>	<i>Structure thickness</i>	<i>SMI</i>
		<i>(mm³)</i>	<i>(mm²)</i>	<i>(1/mm)</i>	<i>(mm)</i>	
Non-neoplastic	<i>Median</i>	0.006	0.178	31.715	0.162	3.372
	<i>Mean</i>	0.018	0.315	44.998	0.167	3.154
	<i>Standard deviation</i>	0.063	0.780	41.464	0.089	0.712
Benign	<i>Median</i>	13.80	106.65	7.73	0.294	1.01
	<i>Mean</i>	94.69	424.68	12.86	0.439	1.28

	<i>Standard deviation</i>	128.24	566.62	10.21	0.321	1.85
Malignant	<i>Median</i>	5.460	37.62	8.42	0.533	3.46
	<i>Mean</i>	45.00	229.01	20.06	0.528	2.20
	<i>Standard deviation</i>	68.13	404.12	29.01	0.356	1.31

Table 4. Summary of the 3D quantitative parameters of microcalcifications, considering malignancy (rounded to three decimal places)

<i>Malignancy</i>		<i>Volume</i> <i>(mm³)</i>	<i>Surface</i> <i>(mm²)</i>	<i>Surface/Volume</i> <i>(1/mm)</i>	<i>Structure thickness</i> <i>(mm)</i>	<i>SMI</i>
Non neoplastic <i>(n=24)</i>	<i>Median</i>	0.006	0.178	31.715	0.162	3.372
	<i>Mean</i>	0.018	0.315	44.998	0.167	3.154
	<i>Standard deviation</i>	0.063	0.780	41.464	0.089	0.712
Benign <i>(n=50)</i>	<i>Median</i>	0.006	0.186	31.091	0.153	3.272
	<i>Mean</i>	0.018	0.319	43.979	0.167	3.240
	<i>Standard deviation</i>	0.031	0.391	45.192	0.090	0.194
Malignant <i>(n=39)</i>	<i>Median</i>	0.022	0.460	19.646	0.234	3.165
	<i>Mean</i>	0.099	1.143	24.279	0.261	3.110
	<i>Standard deviation</i>	0.167	1.480	20.284	0.127	0.316

Figure 1 – Fluoroscopic image of macrocalcification. Note the irregular, fragmented and pleomorphic calcifications. The anatomopathological analysis revealed the presence of a malignant mixed carcinoma.

Figure 2 – Volume rendering of a) A macrocalcification from a malignant mixed-type carcinoma. Clusters of rod-like, V-branched and sometimes pointy objects (179 objects).

Figure 3 – Volume rendering of a) Macrocalcification from a benign lesion (complex adenoma). Note the smooth shape. b) Macrocalcification from a benign lesion (Mixed benign tumour). Note the popcorn-like and spherical objects.

Figure 4 – Three-dimensional representation of: a) Microcalcifications from non-neoplastic glandular tissue. Note the homogeneous, spherical, smooth shaped objects; b) Microcalcifications from malignant lesion (comedocarcinoma) presenting pleomorphism and several rod-like objects.

Figure 5 – Volume rendering of a) Microcalcifications from a benign lesion (simple adenoma); the larger of the objects has a curvy and flattened shape, similar to the teacup shape that may be present in human breast benign lesions; b) Microcalcifications from a benign lesion (complex adenoma); one of the objects has a rod-like shape.

Figure 6 – Box-and-whisker plot representing distribution of the 3D quantitative results for microcalcifications volume and surface/volume ratio, in malignant tumours, benign tumours and non-neoplastic tissue.

Figure 7 - Microphotographs of mammary gland a) Multifocal mineralization in a comedocarcinoma (Hematoxylin & Eosin 50x); b) Multifocal mineralization in a comedocarcinoma (Alizarin Red 50x).

Figure 8 – Microphotographs of mammary gland a) Mineralization of the internal elastic membrane of a muscular artery in non-neoplastic glandular tissue (Hematoxylin & Eosin 50x); b) Mineralization of the internal elastic membrane of a muscular artery in non-neoplastic glandular tissue (Alizarin Red 50x).

Access :
ID : 3802 bo
Name : 3802bo
(C)

HVUE
1

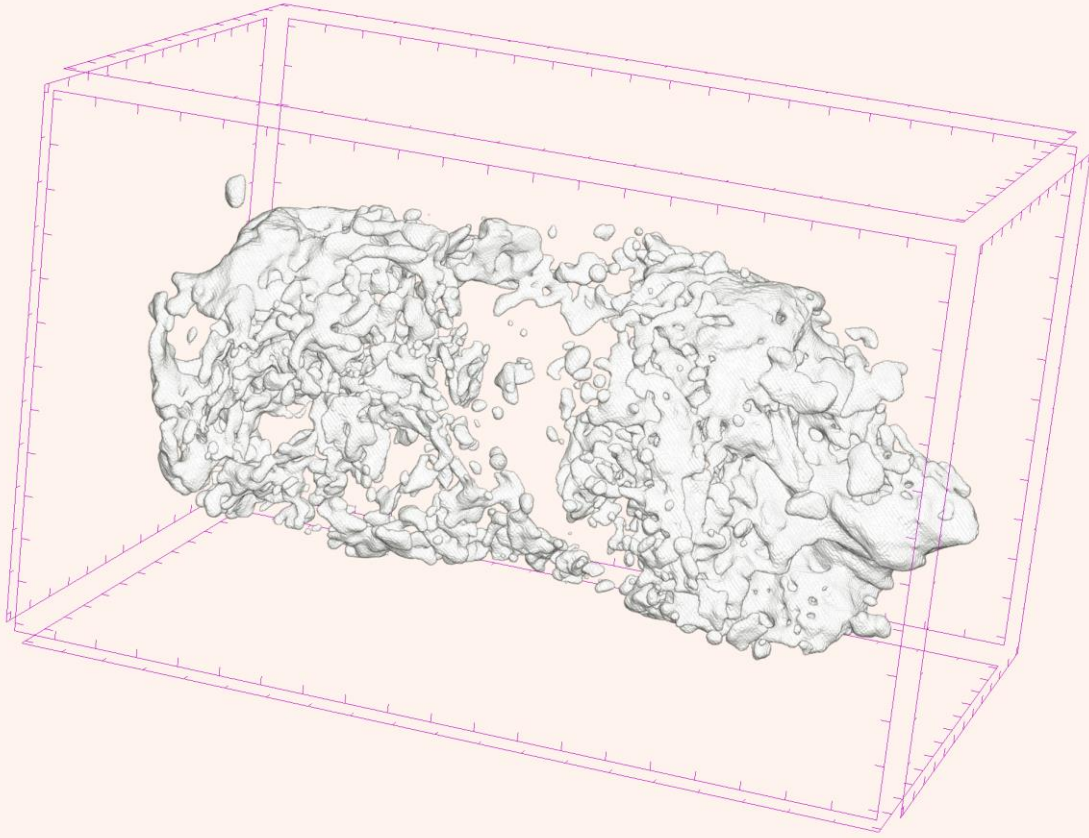


W1: 3
W2: 2.5
2015/02/26-15:29:51

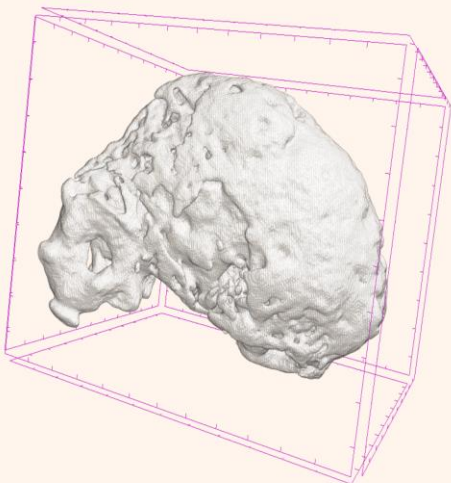
GENORAY



> 1 mm <



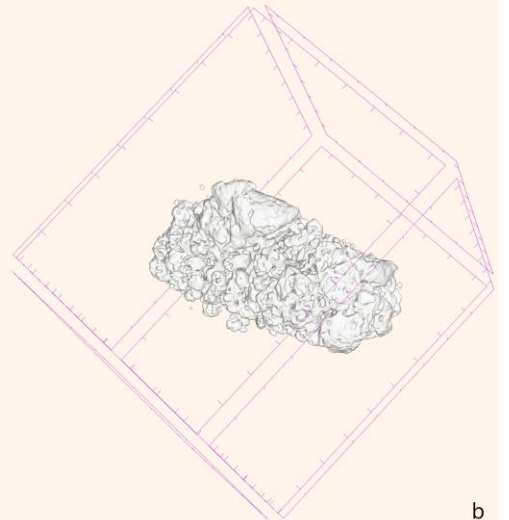
> 1 mm <



a



> 2.5 mm <



b

